

Fermi-Dirac Distribution of Excitons in Coupled Quantum Wells

J. A. Kash, M. Zachau, E. E. Mendez, and J. M. Hong

IBM Research Division, T. J. Watson Research Center, Yorktown Heights, New York 10598

T. Fukuzawa

IBM Research Division, Tokyo Research Laboratory, Sanban-Cho, Tokyo 102, Japan

(Received 4 January 1991)

Time-resolved and cw photoluminescence of excitons in coupled quantum wells with an applied electric field is modeled using a Fermi-Dirac distribution. This distribution can result from inhomogeneous broadening due to interface roughness and the strong, short-range electric dipole repulsion between excitons. The model quantitatively explains the striking temperature dependence of the luminescence linewidth and peak position previously interpreted as a phase transition to an ordered state [T. Fukuzawa, E. E. Mendez, and J. M. Hong, *Phys. Rev. Lett.* **64**, 3066 (1990)]. At very low temperatures ($\lesssim 6$ K), the excitons are in a metastable distribution.

PACS numbers: 73.20.Dx, 78.47.+p, 78.55.Cr, 78.65.Fa

An exciton in a bulk semiconductor or a quantum structure is an electron and a hole which pair up because of their mutual Coulomb attraction. Because both electron and hole are fermions, the exciton is bosonlike. Recently, several experiments have been interpreted in terms of a possible condensation of excitons, in bulk Cu_2O (Refs. 1 and 2) and in coupled quantum wells.³ In a symmetric coupled quantum well with an electric field applied along the growth direction, the electrons and holes separate. This separation reduces the overlap between their respective wave functions, and greatly increases the exciton radiative lifetime.^{4,5} Because of the longer lifetime, it has been suggested that there would be sufficient time for the excitons to come to a condensed, ordered phase.⁶ The recent observation³ of a sharply narrower linewidth of excitons in a coupled quantum well as the temperature was decreased from 12 to 6 K was interpreted as possible evidence for this condensation.

On the other hand, the quantum-well structures grown by modern epitaxial techniques do not result in microscopically smooth heterointerfaces.^{7,8} It has been known for some time that this roughness leads to an inhomogeneous broadening of the excitonic absorption.⁹ Here we show that the excitonic occupation of this inhomogeneous line can be modeled with a Fermi-Dirac distribution. (Using a Fermi-Dirac distribution does not imply that the excitons are fermions. For example, the equilibrium occupation of a set of impurity states follows a Fermi-Dirac distribution if each impurity can trap only a single particle.) Since isolated excitons have boson characteristics, the Fermi-Dirac distribution apparently results from a strong repulsion of the excitons. The repulsion must be large enough that two excitons do not occupy the same spatial position, yet short ranged enough to be neglected for spatially separated excitons. Excitons in coupled quantum wells in an electric field have an electric dipole along the growth direction, and we will show that the repulsion between the dipoles can satisfy these conditions.

The *p-i-n* diode sample used here consists of ten undoped double-quantum-well units separated by 200 Å of $\text{Al}_{0.3}\text{Ga}_{0.7}\text{As}$. Each unit consists of two 50-Å-wide GaAs quantum wells separated by a 40-Å-thick $\text{Al}_{0.3}\text{Ga}_{0.7}\text{As}$ barrier. The layers were grown on an n^+ -type GaAs substrate and capped with 5000 Å of heavily p^+ -type GaAs. For all data reported here, the applied electric field across the quantum-well region was 30 kV/cm. For the time-resolved photoluminescence, electron-hole pairs were generated in the quantum wells by 30-psec laser diode pulses at 1.646 eV, produced at a 5-MHz repetition rate. The energy density at the sample was about 5 nJ/cm² per pulse, resulting in a maximum exciton density of about 10⁹ cm⁻². (As an additional check on density, we observed no screening of the external electric field, implying an exciton density below 10¹¹ cm⁻².) The luminescence was filtered and dispersed in a spectrometer with 0.2-meV resolution, and the kinetics of the luminescence was measured at a series of energies using a photon timing setup¹⁰ with 140-psec full width at half maximum (FWHM) resolution. Luminescence spectra at fixed times after excitation were reconstructed from the kinetics. Each spectrum consisted of a peak arising from the recombination of "indirect" excitons (with electron and hole wave functions mostly confined in different quantum wells). A secondary, very weak feature, peaked at ≈ 1.625 eV, originated from recombination of "direct" excitons (wave functions localized in the same well). Three series of time-resolved spectra for the indirect excitons (the focus of this paper) at different temperatures are shown in Fig. 1.

We first analyze the time-resolved photoluminescence of the excitons to show that the excitonic distribution within the inhomogeneous line is thermal¹¹ at all but the lowest temperatures and that the Fermi-Dirac distribution can be used to model the data accurately. During the first few nanoseconds, the exciton kinetics is quite complex. The free carriers generated by the laser relax into excitons,¹² the kinetic energy of each exciton is reduced to $\approx kT$ by interactions with phonons,¹² the direct

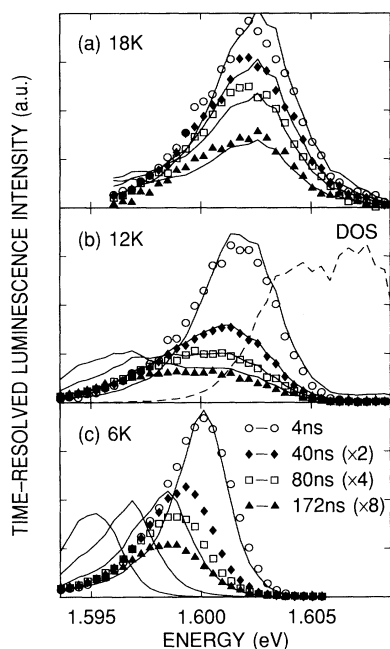


FIG. 1. Photoluminescence spectra of the indirect excitons in a coupled quantum well for various delay times at three different temperatures. The delay times and their relative scalings are the same for each temperature, and are indicated in (c). Solid curves are the calculated spectra, derived as explained in the text, while the symbols are the measured spectra. The dashed curve in (b) is the density of states (DOS) used in all calculations. The fine structure in this DOS results from noise in the measured spectra.

excitons relax into indirect excitons,⁵ and the excitons drift into the low-energy regions of the quantum wells.¹³ In a conventional single quantum well or a coupled well with no applied fields, the exciton lifetime is typically less than a nanosecond,^{5,14,15} and so the excitons have all recombined before this part of the kinetics ends. Because of the much longer lifetime of excitons in the coupled wells with an applied field,^{4,5} one can observe the excitons well after this short-time relaxation. At longer times, such as those displayed in Fig. 1, it might be possible for the excitons to occupy the inhomogeneous distribution in quasithermal equilibrium.¹¹ Analysis of the 18-K spectra indicates that this is indeed the case. For 18 K and higher temperatures, the spectral shape is stationary with time, while the intensity decreases monotonically with time as the excitons recombine. Because the distribution is independent of density, the classical Maxwell-Boltzmann (MB) distribution is evidently a good approximation at these higher temperatures. If the density of states (DOS) representing the spatial dependence of the exciton energy is $D(E)$, with E the exciton energy, then for the MB distribution

$$N(E,t) \propto D(E) \exp(-E/k_B T), \quad (1)$$

where $N(E,t)$ is the exciton density at energy E and

time t . $N(E,t)$ is proportional to the experimentally measured luminescence intensity $I(E,t)$.

From Eq. (1) and the spectra at 18 K in Fig. 1(a), one can derive $D(E)$. Then one can predict the spectrum at any other temperature again using Eq. (1). For $T > 18$ K, Eq. (1) gives a good agreement with the data. At lower temperatures, however, the MB distribution clearly does not apply, as the measured spectra change shape with time, that is, with integrated exciton density. For the Bose-Einstein (BE) distribution function, the chemical potential μ must be at a lower energy than any exciton state so that the distribution function is always non-negative. The low-energy tail of the DOS extends below 1.592 eV, while the luminescence at 12 K is primarily at $E > 1.597$ eV. For $E > 1.597$ eV, $(E - \mu)/k_B T > 5$, so that $E > 1.597$ eV corresponds to the high-energy tail of the BE distribution. Therefore the BE distribution function in this range will be essentially identical to the MB distribution function. Since neither distribution can model the low-temperature data, we try instead to fit the data with a Fermi-Dirac (FD) distribution, i.e.,

$$N(E,t) = D(E) f(E, \mu, T), \quad (2)$$

where $f(E, \mu, T) = \{\exp[(E - \mu)/k_B T] + 1\}^{-1}$ is the FD distribution function. The chemical potential μ is implicitly a function of temperature and density. For the time-resolved spectra, the integrated exciton density changes with time and longer times correspond simply to lower densities. The corresponding change in μ is determined by

$$\int D(E) f(E, \mu, T) dE \propto \int I(E, t) dE \quad (3)$$

for each time t . Equation (3) expresses the requirement that the measured integrated luminescence intensity is proportional to the calculated integrated exciton density. Because μ cannot be independently measured, $D(E)$ cannot be determined from Eq. (2) using a single measured spectrum. Instead, we iteratively determine μ and $D(E)$ from the 12-K data at 4 and 40 nsec. An initial guess for μ at 40 nsec is made, and Eq. (2) is then used to determine a DOS from the 40-nsec data. The predicted 4-nsec spectrum is then calculated from this DOS, where μ at 4 nsec is determined from Eq. (3). The initial guess for μ at 40 nsec is then varied until a satisfactory spectrum at 4 nsec is obtained. The DOS obtained from this procedure is shown in Fig. 1(b), and will be used as $D(E)$ in all subsequent calculations. All other time-resolved spectra may be calculated from this DOS using Eqs. (2) and (3) without additional adjustable parameters. As seen in Figs. 1(a) and 1(b), this procedure gives good results for $T \geq 12$ K, except at the lowest exciton energies $E \lesssim 1.598$ eV. For the 6-K spectra (where much of the luminescence is at these lowest energies), the calculated variation with times does not match the measurements. Except for these low energies and temperatures, a FD distribution seems to be a good choice for the data. The deviations will be discussed below.

Further support for the Fermi-Dirac distribution comes from cw luminescence spectra. As reported earlier,³ there is a striking change of spectral width and peak position with temperature as shown in Fig. 2.¹⁶ For these data, the intensity of the 1.657-eV cw dye laser is held constant at 0.1 W cm^{-2} . Because the photoluminescence decay time⁵ is a nearly constant 40 nsec throughout this temperature range, the exciton density in the cw experiments is constant at about $3 \times 10^8 \text{ cm}^{-2}$. To model the cw data, μ is first adjusted to fit the 12-K data using the DOS of Fig. 1(b). The change in μ with temperature is then determined by requiring $\int N(E)dE$ to be constant with temperature. The predicted change in spectral shape and width are shown in Fig. 2, as is the calculated change in μ . Except for temperatures below 6 K, the quantitative agreement between the model and the data is excellent. Changes in density, particularly around 12 K, produce significant changes in the measured spectra for exciton densities several times higher or lower than the data of Fig. 2. These changes are accurately predicted by the model.

The striking changes in the spectra of Fig. 2 can be understood by examining the temperature variation of the chemical potential $\mu(T)$ at constant density. Expanding $\mu(T)$ about $\mu(0)$ gives the result¹⁷

$$\mu(T) = \mu(0) - \frac{\pi^2}{6} (k_B T)^2 \left(\frac{d \ln D(E)}{dE} \right)_{E=\mu(0)} \quad (4)$$

In conventional fermion systems such as metals or partially filled valence or conduction bands in semiconductors, $D(E)$ changes slowly around $\mu(0)$, so μ changes slowly with T . In the low-energy tail of a Gaussian or other similarly broadened DOS, $D(E)$ increases approximately exponentially with E and therefore μ changes rapidly, as can be seen in Fig. 2(b). In fact, although μ in Fig. 2(b) is not derived using Eq. (4), it is in reasonable agreement with Eq. (4). For temperatures below about 12 K, the chemical potential is near the peak of the luminescence and the FD distribution must be used to accurately model the data. For temperatures above 18 K, μ is in the low-energy tail of the luminescence, and so the MB distribution is a reasonable approximation. Thus, the large change in spectral width and peak position result directly from the rapid decrease in $\mu(T)$.

The FD distribution is clearly a good model for the data. We now consider why this distribution might apply to these excitons. It is important to recall that the GaAs/Al_{0.3}Ga_{0.7}As interface is not perfectly smooth, and that the roughness leads to inhomogeneous broadening of the exciton line.⁷⁻⁹ The spatial scale of the roughness is not critical here; we require only that different spatial positions in the quantum-well plane correspond to different energies.¹⁸ In our heterostructure, roughness of one monolayer corresponds to an inhomogeneous width of about 6 meV, in reasonable agreement with the width of the calculated DOS. In a coupled quantum well with

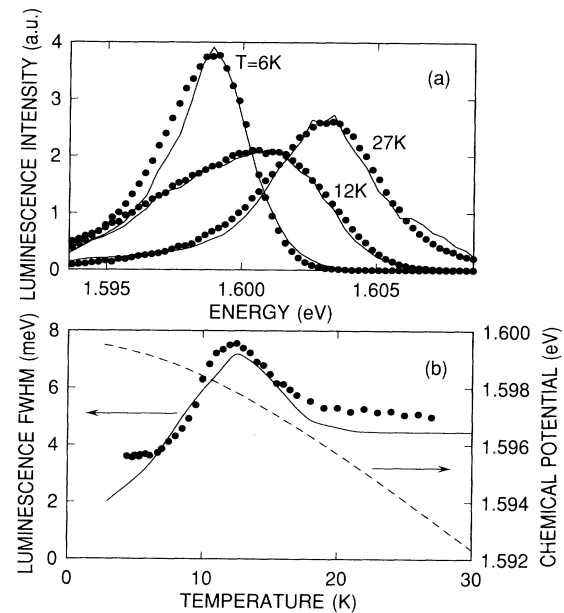


FIG. 2. (a) Measured (points) and calculated (lines) cw photoluminescence spectra at three different temperatures. The laser intensity is the same for all data; the calculations assume a constant exciton density. The density of states is shown in Fig. 1(b). (b) Measured and calculated full width at half maximum for the set of spectra represented in (a). The dashed curve is the calculated variation in the chemical potential with temperature.

an applied electric field, the excitons have an electric dipole along the growth direction, corresponding in this sample to an electron-hole separation of about 100 Å. As a result of this dipole, there is a strong short-range repulsion between excitons, amounting to 1.3 meV for a 200-Å exciton separation, and 7.0 meV for a 100-Å separation. In the absence of interactions between the excitons, BE statistics would apply, and in equilibrium most of the excitons would occupy states within $\approx kT$ of the chemical potential. Such states represent only a tiny fraction of the area of the quantum-well plane, so that the density of excitons in these areas of lowest energy would be orders of magnitude higher than the average density. Because of the strong dipole repulsion of the excitons, in equilibrium the excitons will spread out to other areas (of higher energy) in the quantum-well plane. Because the excitons are avoiding each other, the FD distribution gives a good noninteracting-particle approximation to the equilibrium configuration. An exact solution will require details about the scale of interface roughness and the actual distance dependence of the repulsion, and so will be much more complex. By using the FD distribution, we approximate the repulsion by a step function. The repulsion is assumed to be greater than the luminescence linewidth for excitons separated by \lesssim (an exciton radius) and zero for larger separations. This approximation means that the potential energy of

one exciton is not altered by the presence of other excitons, except that no two excitons occupy the same spatial position.

It may seem that the deviations from the FD distribution seen in Fig. 1(c) and at low temperatures in Fig. 2(b) weaken the evidence for our model. We now show that the excitons can be in a metastable distribution at these low temperatures, and that this metastability is a natural consequence of our model. We have noted that the interface roughness leads to a position-dependent exciton energy. As a result, there will be "barriers" and "valleys" in the exciton energy as a function of position. In order for the DOS to be occupied in thermal equilibrium, an exciton must be able to move by thermal activation from one valley to another within its lifetime. Because of interactions with phonons, each exciton has kinetic energy $\approx kT$,¹² corresponding to a thermal velocity $v_{\text{th}} = 10^6$ cm sec⁻¹ at 6 K. The probability that an exciton is thermally activated over a barrier of height ΔE on any single attempt is $\approx \exp(-\Delta E/kT)$, while the attempt frequency is roughly v_{th}/W , where W is the distance between barriers. Therefore, the typical time for an exciton to get over a barrier is

$$t \approx (W/v_{\text{th}})e^{\Delta E/kT}. \quad (5)$$

Because of the exponential variation of t with ΔE , and because neither ΔE nor W is accurately known, we can only estimate this time. Choosing a typical barrier height as half the width of the DOS, $\Delta E \approx 3$ meV, and taking $W = 2000$ Å, Eq. (5) gives $t \approx 8$ nsec, which is of the same order of magnitude as the 40-nsec exciton lifetime. Clearly, below some temperature excitons will become trapped in valleys, and will not be able to occupy the DOS thermally. Because of the exponential dependence in Eq. (5), this metastable trapping will occur below a threshold temperature. Then, the luminescence will stop changing with decreasing temperature, as is observed in Fig. 2(b) for temperatures below 6 K. The metastability is also seen in Fig. 1(c), where the observed changes with time are much smaller than predicted by the thermal model.

Excitons in this coupled quantum well occupy a density of states which is inhomogeneously broadened by interface roughness. Repulsion between excitons results in a Fermi-Dirac distribution when the temperature is high enough that excitons can be thermally activated over the potential barriers. A large increase with energy in the density of states around the chemical potential leads to striking changes in the luminescence spectrum as a function of temperature or exciton density. The dipole interaction of these excitons provides one source of repulsion. With no applied field, there is no first-order dipole repulsion of excitons in either coupled or single quantum wells. On the other hand, there are still interactions between excitons. A second-order dipole repulsion and, at high densities, phase-space filling will cause excitons to repel each other. One may therefore speculate on the ex-

citon distribution in the absence of an electric field. However, because of the short exciton lifetimes in the absence of a field, the excitons do not reach quasiequilibrium. In addition, as heterointerface qualities are improved, the inhomogeneous linewidth will decrease. Finally, at high densities, screening of the external field and also the possibility of an electron-hole liquid will need to be considered. Studying the thermodynamics in these regimes remains a challenge.

We thank Antigoni Alexandrou for useful discussion and assistance with the experiments, and Malcolm Christie for preparation of the *p-i-n* diodes. We are grateful to Alan Fowler, Dung-Hai Lee, Frank Stern, and Eizaburo Yamada for helpful discussions.

¹D. W. Snoke, J. P. Wolfe, and A. Mysyrowicz, *Phys. Rev. Lett.* **64**, 2543 (1990).

²D. Snoke, J. P. Wolfe, and A. Mysyrowicz, *Phys. Rev. B* **41**, 11171 (1990).

³T. Fukuzawa, E. E. Mendez, and J. M. Hong, *Phys. Rev. Lett.* **64**, 3066 (1990).

⁴S. Charbonneau, M. L. Thewalt, E. S. Koteles, and B. Elman, *Phys. Rev. B* **38**, 6287 (1988); J. E. Golub, K. Kash, J. P. Harbison, and L. T. Florez, *Phys. Rev. B* **41**, 8564 (1990).

⁵A. Alexandrou, J. A. Kash, E. E. Mendez, M. Zachau, J. M. Hong, T. Fukuzawa, and Y. Hase, *Phys. Rev. B* **42**, 9225 (1990).

⁶T. Fukuzawa, S. S. Kano, T. K. Gustafson, and T. Ogawa, *Surf. Sci.* **228**, 482 (1990).

⁷C. Weisbuch, R. Dingle, A. C. Gossard, and W. Weigmann, *Solid State Commun.* **38**, 709 (1981).

⁸A. Ourmazd, D. W. Taylor, J. Cunningham, and C. W. Tu, *Phys. Rev. Lett.* **62**, 933 (1989).

⁹J. Hegarty, M. D. Sturge, C. Weisbuch, A. C. Gossard, and W. Wiegmann, *Phys. Rev. Lett.* **49**, 930-932 (1982).

¹⁰V. J. Koester and R. M. Dowben, *Rev. Sci. Instrum.* **49**, 1186 (1979).

¹¹Thermal occupation of the density of states is not the same as an exciton being in equilibrium with the lattice. Equilibrium with the lattice simply means that the average kinetic energy of the exciton is kT .

¹²T. C. Damen, J. Shah, D. Y. Oberli, D. S. Chemla, J. E. Cunningham, and J. M. Kuo, *J. Lumin.* **45**, 181-185 (1990).

¹³M. Zachau, J. A. Kash, and W. T. Masselink (unpublished).

¹⁴J. A. Kash, E. E. Mendez, and H. Morkoç, *Appl. Phys. Lett.* **46**, 173 (1985).

¹⁵H. J. Polland, L. Schultheis, J. Kuhl, E. O. Göbel, and W. T. Tu, *Phys. Rev. Lett.* **55**, 2610 (1985).

¹⁶To account for sample heating by the cw laser and thermometry errors (different cryostats were used for cw and time-resolved measurements), the temperature is taken to be 2 K higher than the measured temperature for the cw data.

¹⁷N. M. Ashcroft and N. D. Mermin, *Solid State Physics* (Holt, Rinehart and Winston, New York, 1976), pp. 46 and 47.

¹⁸This random variation of potential with position is an essential difference between this system and a gas of hard-sphere bosons, e.g., liquid helium.